PRAMANA — journal of physics

Vol. 80, No. 4
April 2013
pp. 607–619

Energy-dispersive X-ray diffraction beamline at Indus-2 synchrotron source

K K PANDEY*, H K POSWAL, A K MISHRA, ABHILASH DWIVEDI, R VASANTHI, NANDINI GARG and SURINDER M SHARMA

High Pressure & Synchrotron Radiation Physics Division, Bhabha Atomic Research Centre, Trombay, Mumbai 400 085, India
*Corresponding author. E-mail: kkpandey@barc.gov.in

MS received 5 March 2012; revised 29 August 2012; accepted 8 October 2012

Abstract. An energy-dispersive X-ray diffraction beamline has been designed, developed and commissioned at BL-11 bending magnet port of the Indian synchrotron source, Indus-2. The performance of this beamline has been benchmarked by measuring diffraction patterns from various elemental metals and standard inorganic powdered samples. A few recent high-pressure investigations are presented to demonstrate the capabilities of the beamline.

Keywords. Synchrotron beamlines; X-ray diffraction; high pressure.

PACS Nos 07.85.Qe; 62.50.−P; 61.05.cp

1. Introduction

X-ray diffraction technique [1,2] is the most widely used technique for investigating the structure of materials under various thermodynamics conditions, viz. temperature and pressure. There are two variants of the X-ray diffraction technique, viz. angle-dispersive X-ray diffraction (ADXRD) and energy-dispersive X-ray diffraction (EDXRD) [3–6]. In angle-dispersive method, the monochromatic X-ray beam is incident on the sample and the diffraction pattern is recorded as a function of angle (θ) whereas in energy-dispersive method, the sample is exposed to the white X-ray beam and the diffracted X-rays are energy analysed at a fixed angle. EDXRD technique is particularly useful in situations where temporal evolution of the sample is of relevance or the measurements require constrained geometry, such as for samples at high pressures and/or high temperatures etc. Unlike area detectors used for ADXRD variant where diffraction pattern can be seen only at the end of the measurement, the usage of energy-sensitive detector with multichannel analyser in EDXRD technique literally permits online viewing of the whole diffraction pattern while collecting data. This feature of EDXRD method makes it better suited for kinetics studies. Generally, the EDXRD method provides data over a larger Q ($= 2\pi/d$)

DOI: 10.1007/s12043-012-0493-0; ***e*Publication: 23 February 2013**

range, as here the Q range is defined by energy range of the white synchrotron radiation and the collection angle (θ). This can provide better real-space structural resolution.

For the EDXRD method, Bragg condition is re-written as

$$Ed_{hkl} \sin\theta = 6.1999, \tag{1}$$

where E is the energy of the X-ray photons (in keV) satisfying the Bragg condition for the hkl planes having interplaner distance of d_{hkl} (in Å) at a diffraction angle θ [7]. The inverse relation between E and d_{hkl} implies that if X-rays of large energy are available, then the diffraction from small d values can be recorded, resulting in larger Q range. Synchrotron, being an intense source of X-rays with a very broad spectrum, fulfills this requirement. In addition to this, several unique experiments are possible only with EDXRD method like detecting diffraction peaks corresponding to charge density wave (CDW) by chemically filtering the Bragg peaks [8]. Diffraction from CDW is usually very weak and is hardly observable in ADXRD measurements.

We have designed and developed an EDXRD beamline at BL-11 port of the recently commissioned Indian synchrotron source, Indus-2. This synchrotron, situated at Raja Ramanna Centre for Advanced technology, Indore, India, is designed to operate at 2.5 GeV electron bunch energy and 300 mA of storage current [9]. EDXRD beamline utilizes white synchrotron radiation (SR) from a bending magnet, filtered through 200 μm thick water-cooled Be window and collimated using various precision slits. Diffracted X-rays from the sample are energy analysed using high purity germanium (HPGe) detector. With white SR beam from bending magnet having reasonable intensity up to 70 keV and a wide range of 2θ angle selectivity of $\pm 25^\circ$, one can record the diffraction data over a large Q range (up to 15 Å^{-1}) at this beamline.

Presently, this beamline has been installed at the bending magnet port. However, the design parameters of various components have been finalized such that it can be easily shifted in future to any insertion device port such as wiggler or wavelength shifter without any alteration. In that sense, this beamline is at par with any other energy-dispersive beamline installed at advanced synchrotron sources worldwide, for example 16-BM-B beamline at Advanced Photon Source (USA), BL04B1 at SPring8 (Japan), 7T-MPW-EDD1 beamline at BESSY-II (Germany) etc. [10–12].

In order to investigate the performance of this beamline, we have carried out several benchmarking experiments of various elemental metal foils and powdered samples. One such measurement on Au foil is presented here to give an idea of the detector and geometrical resolution. A few recent high-pressure investigations at this beamline are also presented in this communication in order to show the beamline capabilities.

2. Description of EDXRD beamline

The beamline comprises water-cooled Be window, 6 mm Cu beam stopper, water-cooled motorized primary slit system, evacuation port, precision slit system, ionization chamber, collection slits mounted over various motorized stages, HPGe detector and 8-axes motorized goniometric stage with the provision of alignment of entire experimental station with respect to SR beam and sample maneuverability in x, y, z, θ and χ directions. White

SR beam from a bending magnet port with a horizontal fan of 1 mrad is accepted at Be window which removes the unwanted low-energy portion (<3 keV) of SR spectrum. It also separates the vacuum of storage ring from that of the beamline. Water-cooled primary slit system is used to select the central collimated portion of SR beam. The beam size is further reduced to restrict the gauge volume (diffraction volume) to the size of the sample. Diffraction data are collected with the help of the HPGe detector at a fixed 2θ angle defined by two collection slits. In addition to defining the diffraction angle, these slits remove Compton scattered background. Design parameters of various components and the mechanical lay-out of EDXRD beamline are described below.

2.1 *Design*

As SR beam coming from the bending magnet is plane polarized in horizontal plane i.e. the plane of storage ring, the diffraction data collected in vertical plane does not suffer from intensity loss due to polarization. However, designing energy-dispersive beamline with 2θ angular maneuverability in vertical plane, is far more demanding from the mechanical point of view especially when the detector is liquid nitrogen cooled. If we consider collection angle in the horizontal plane as large as 25°, the diffraction intensity is reduced by <20% only. With these considerations, the EDXRD beamline at BL-11 is designed to collect energy-dispersive data in the horizontal plane. The key parameters which play important roles in the overall performance of beamline are the size and divergence of incident SR beam, the geometrical resolution of the collection system and the detector resolution. The first two parameters are discussed in the optical design part of this section and the other parameters are discussed in the experimental part.

2.1.1 *Optical design.* Low divergence of incident beam is one of the basic characteristics of synchrotron radiation. It is known to vary as $1/\gamma$ where $\gamma = (m/m_0) = 1/\sqrt{(1-\beta^2)}, \beta = v/c$ [13]. For Indus-2, γ is ∼5000 which corresponds to a divergence of ∼0.2 mrad. The horizontal divergence is controlled by the sweep of emitted X-rays across the width of the first slit. For EDXRD beamline first slit, called primary slit system, is at ∼16000 mm from the tangent point of the source which means a slit opening of 3.2 mm for 0.2 mrad divergence. However, since SR beam profile is Gaussian and high-energy X-rays are more concentrated in the central region (i.e. around 0°), the SR beam needs to be further cut down in order to select the central flat portion with high-energy photons. With these requirements, primary slit system for EDXRD beamline has been designed to define the size of SR beam controlled by four independent jaws [14] (figure 1a). Vertical jaw movement ranges from −2 mm to 15 mm whereas horizontal jaw movement ranges from −2 mm to 30 mm. All the motions are actuated using stepper motors with a resolution and repeatability of 1 μm. Whole slit assembly resides in UHV compatible chamber. Slits are made from 5 mm tungsten carbide plates. Since this is the first component of the beamline, all the slit blades are water-cooled to take care of the head load of SR beam which is ∼30 W/mrad.

The size of 1 mrad (horizontal) SR beam at the primary slit is ∼5 mm × 18 mm out of which only 500 × 500 μm central beam is selected. It is further cut down in order to restrict the gauge volume with the help of precision slit system shown in figure 1b. This is

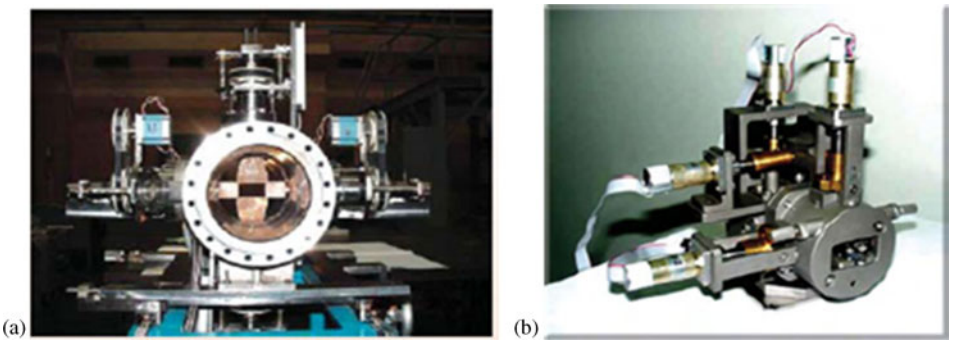

Figure 1. (**a**) Primary slit system, (**b**) precision slit system.

particularly required for high-pressure experiments employing diamond anvil cells (DAC) [15] where the sample chamber is of the order of 150 μm or smaller. The precision slit system is based on flexure design. So there is no sliding motion and hence no friction between mating parts, which makes the system very accurate. Slit assembly has two identical four-bar mechanisms [16]. The shape of the opening of the slit can be made either square or rectangular, as needed, and its range is from 0×0 μm^2 (completely closed) to 200×200 μm^2, with a resolution of 0.06 μm. Two of these slits are used to finally define the SR beam of size less than 100×100 μm^2 at the sample with vertical and horizontal divergence <6 μrad.

For high-pressure measurements, the beam size can be further reduced with the help of Kirkpatrick–Baez (KB) mirror system without compromising the flux [17]. This consists

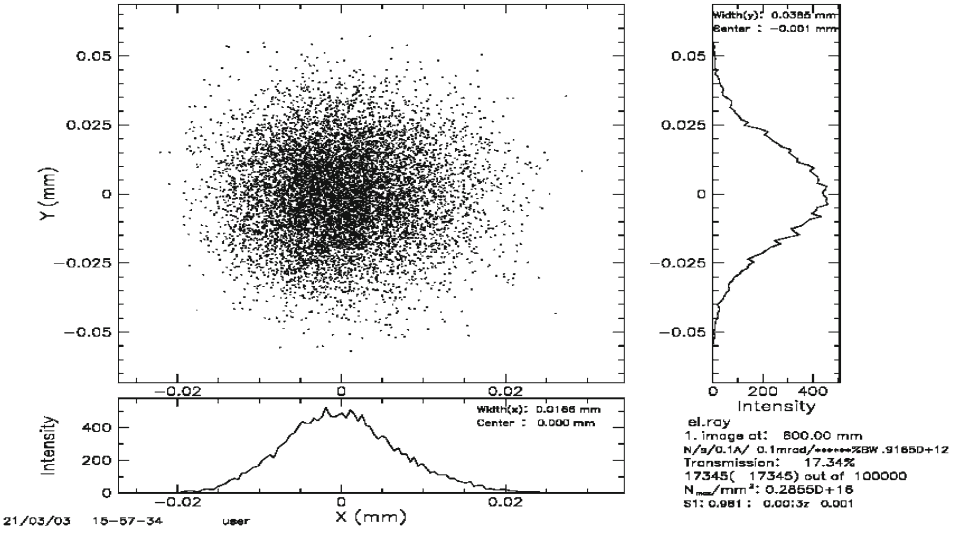

Figure 2. Ray tracing simulation of focal spot size using a KB mirror system.

of a set of two mirrors which focus the SR beam in horizontal and vertical directions. We have carried out ray tracing simulations using SHADOWUVI [18] software incorporating all the slits and KB system. Our simulations show that a spot size of <30 μm diameter can be achieved at the samples with 200 μm $\times$ 200 μm precision slit opening (figure 2) which means a flux gain of about two orders of magnitude at the sample if similar spot size were to be selected using only the slits. A provision has been kept in the beamline design to incorporate KB mirror system when it becomes available.

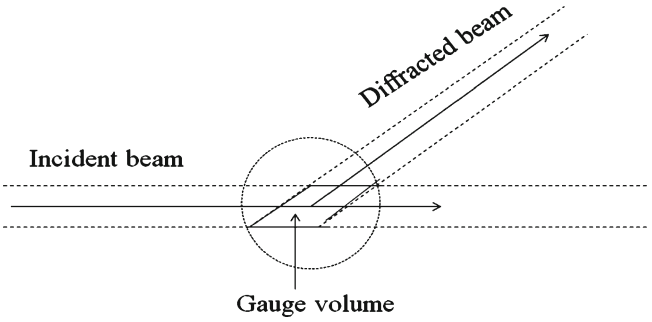

Figure 3. Gauge volume.

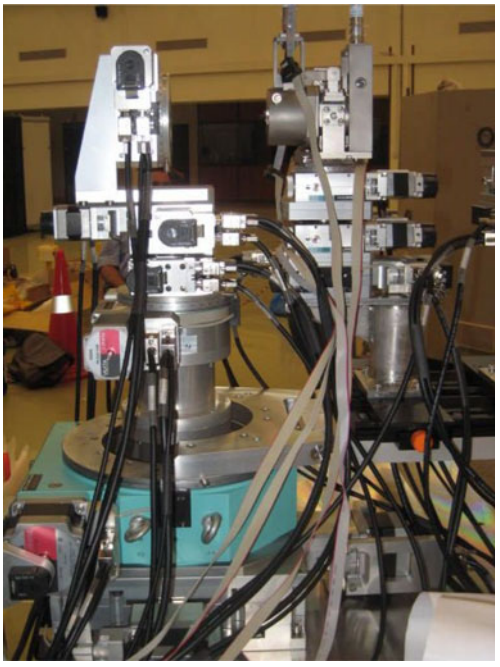

Figure 4. Sample stage goniometer.

2.1.2 *Experimental station.* Primary requirement in designing experimental station is to have provision for the alignment of sample with respect to the synchrotron beam and selectivity of diffraction angle with an optimum resolution. Another most important thing is to bring the sample precisely at the gauge volume. Gauge volume is the diffraction volume defined by the incident beam and the diffracted beam (figure 3).

To meet these requirements, an eight-axes goniometric sample stage has been used. It comprises a pair of linear translational XY stages at the bottom, 2θ rotational stage with detector arm supported by airpads, θ stage, and XYZχ stages at the top (figure 4). Bottom XY stage is used for 2θ axis alignment with respect to the synchrotron beam. θ stage, whose axis coincides with 2θ stage, is used for sample rotation. Upper XYZ stages provide maneuverability in parallel and perpendicular directions with respect to the beam. χ stage provides rotation about an axis perpendicular to the 2θ axis. The purpose of this stage is to have an additional capability of carrying out single crystal Laue diffraction. All the stages above 2θ stage are used for sample positioning at the gauge volume. Since our precision requirements for sample allignment are quite stringent, all these motorized stages have translational resolution at a few micron level.

The 2θ stage and the two precision slits mounted over the detector arm are used to define diffraction angle. The diffraction angle can be selected in the range of $\pm 25^\circ$. Liquid nitrogen-cooled HPGe detector which is also mounted on the detector arm is used for diffraction measurement. The weight of the detector and the slit systems is supported by air pads which provide smooth motions of the detector arm with negligible load at 2θ stage.

2.2 *Mechanical lay-out*

Mechanical lay-out of EDXRD beamline is shown in figure 5. Figure 6a is the photograph of the installed beamline. As described earlier, the SR beam is transported to the sample through a Be window, primary and precision slit systems. SR beam remains in vacuum (10^{-5} torr) till the precision slit system to minimize the loss of X-ray intensity due to air scattering. The diffracted beam from the sample is collected at a chosen 2θ angle with the help of HPGe detector.

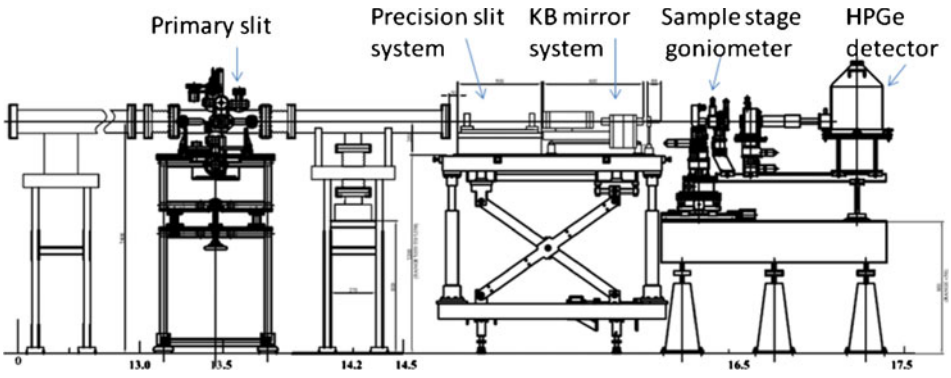

Figure 5. Mechanical lay-out of EDXRD beamline.

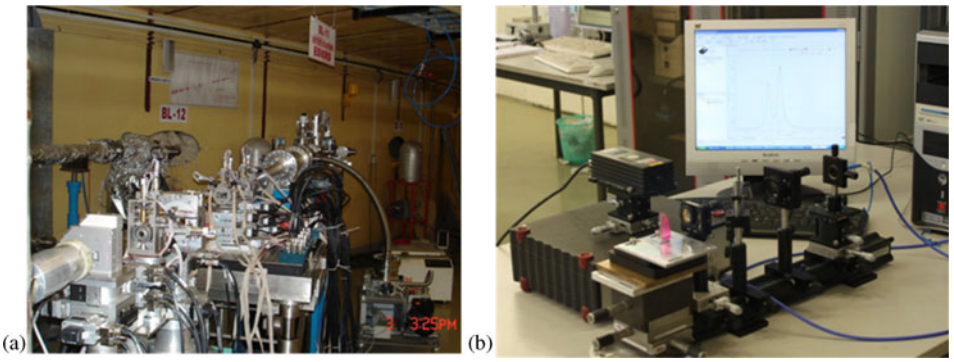

Figure 6. (**a**) EDXRD beamline, (**b**) off-line ruby pressure measurement set-up.

For *in-situ* high-pressure experiments, pressure inside a DAC can be monitored using an equation of state of internal pressure calibrant e.g. Au, Cu etc. [19]. Since the diffraction peaks from these often interfere with the sample diffraction peaks, a preferred method for the pressure measurement is based on the shift of ruby R-lines. For this, a tiny ($\sim$10 μm) particle of ruby is loaded along with the powdered sample inside a DAC [20]. To facilitate the use of ruby fluorescence method we have developed and installed a set-up comprising 532 nm frequency doubled diode pumped solid-state laser, microscope objective and optical fibre coupled portable spectrometer (figure 6b).

2.3 *Shielding and automation of EDXRD beamline*

To ensure that the experimenters are not exposed to unwarranted radiation, the synchrotron beamlines at high-energy synchrotron sources are required to be properly shielded. Primarily, there are two types of radiations, viz. high-energy Bremsstrahlung radiation (BR) ranging from a few keV to GeV and the low-energy scattered synchrotron radiation (<25 keV). BR is mostly limited in forward direction within 15° cone at scattering locations whereas low-energy scattered SR is more prominent at higher angles. Shielding requirement becomes more stringent for white beams especially when SR beam is taken out in air for experiments. For these reasons, the whole EDXRD beamline is covered by a shielding hutch made of 3 mm Pb sheet sandwiched between 1.5 mm MS sheets [21]. BR is locally shielded covering 15° cone using Pb blocks of thickness $\sim$10 cm at the first scattering location (primary slit). One more local shielding of 10 cm thick Pb blocks is placed at the end of the beamline. The shielding hutch door is radiation interlocked to rule out any accidental radiation exposure.

In order to remotely control and operate the beamline, all the beamline components are motorized and automated. A scanning program is written to align the sample to the gauge volume. This spirally scans the sample in YZ plane (perpendicular to SR beam) and the beam transmission through the sample is monitored using Si photodiode and Keithley picoammeter. This is especially helpful in the case of high-pressure experiments using DAC. The scan is displayed in pixilated form where each pixel represents the intensity at a particular YZ position. Correct X position of the sample along SR beam is iteratively determined by θ scan.

3. Benchmarking

Performance of EDXRD beamline has been investigated by analysing diffraction patterns from various elemental metal foils and powdered sample. First set of benchmark EDXRD patterns of several elemental metals, viz. Au, Cu, W, Ta, Zr, Mo etc., were recorded in May, 2008. As an example, diffraction pattern of Au foil and the obtained geometrical and detector resolution parameters are presented here (figure 7, table 1).

Characteristic X-ray fluorescent peaks from Au foil give the detector a resolution of about 2%. Resolution of the diffraction peak is the convolution of the detector and the geometrical resolution which depends on the incident beam size and slit width of the collection slits.

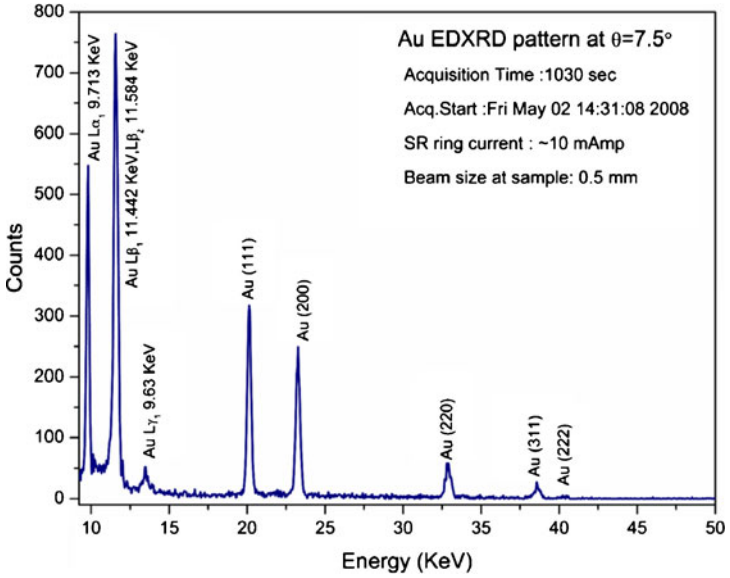

Figure 7. A powder diffraction pattern of Au foil recorded at EDXRD beamline.

Table 1. Energy resolutions of various diffraction and X-ray fluorescence peaks.

Peak details	$\Delta E/E$
Au Lα_1 (9.713 keV)	0.021
Au Lβ_1 (11.442 keV), Au Lβ_2 (11.584 keV)	0.026
Au(1 1 1)	0.014
Au(2 0 0)	0.013
Au(2 2 0)	0.012
Au(3 1 1)	0.011

By the differentiation of Bragg equation (eq. (1)) under the assumption that δE and $\delta\theta$ are the errors of the measurements of photon energy and Bragg angle respectively, and are of statistical nature, one obtains

$$\frac{\delta d}{d} = \left[\left(\frac{\delta E}{E}\right)^2 + (\cot\theta\delta\theta)^2\right]^{1/2}, \tag{2}$$

where δd is the absolute precision of the interplaner spacing measurement. $\delta\theta$ is usually $\sim 10^{-4}$ radians or smaller. For diffraction angle $\theta = 7.5°$, second term in the right-hand side is smaller than 10^{-2}. δE depends on two parameters, viz. the energy resolution of the detector, δE_{D}, and the energy broadening of the reflection due to the beam divergence δE_θ.

$$\delta E = \left[(\delta E_{\mathrm{D}})^2 + (\delta E_\theta)^2\right]^{1/2}. \tag{3}$$

Since beam divergence is of the order of microradians, δE is comparable to δE_{D}. Our peak analysis of diffraction peaks show that diffraction resolution is also $\sim$2% which is quite comparable to the detector resolution implying that the only limiting factor is the detector resolution. Nevertheless, this is comparable to the resolution of other EDXRD beamlines across the world.

Due to the inherent computational difficulty in the Rietveld refinement [22] of the energy-dispersive diffraction pattern, it is not yet implemented in any of the widely used

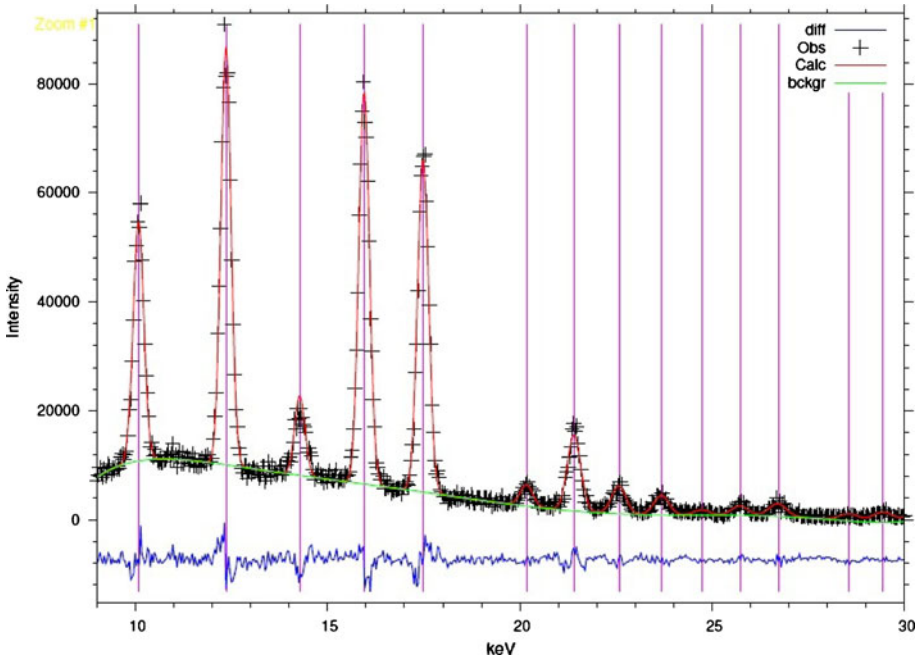

Figure 8. Le Bail refinement of energy-dispersive diffraction pattern of LaB_6.

refinement softwares such as GSAS [23] etc. However, the lattice parameters can be easily refined using Le Bail method [24]. We are presenting here the Le Bail refinement of LaB_6 lattice parameter (figure 8) carried out using GSAS software. The energy-dispersive diffraction data of the powdered LaB_6 sample were recorded under ambient conditions. The refined value of lattice parameter is found to be 4.153(1) Å which is close to the earlier reported value (4.1527 Å) [25]. These measurements show that this beamline can be used for structural investigations of materials and the lattice parameters can be refined with a reasonable accuracy.

4. Recent experiments

The EDXRD beamline is now being routinely used for sample characterization under ambient conditions and for carrying out high-pressure EDXRD experiments. A few recent high-pressure studies using this beamline are discussed below.

4.1 *Equation-of-state measurement of elemental metals, viz. Au and Cu*

Equation-of-state (EOS) of elemental metals such as Au, Cu etc. are generally used as pressure calibrants for *in-situ* high-pressure X-ray diffraction experiments. In order to reproduce the EOS of these standard pressure calibrants, we carried out high-pressure EDXRD measurements on these metals up to the hydrostatic pressure limit of ethanol–methanol pressure transmitting medium. For pressure calibration, ruby chip of size less than 20 μm was loaded in DAC along with powdered sample and pressure transmitting medium. Using second-order Birch–Murnaghan equation-of-state [26] we found the bulk modulus of Au and Cu to be 172 $\pm$ 2 GPa and 135 $\pm$ 2 GPa respectively (figure 9) which is in close agreement with the earlier reported values, viz. 167 GPa and 133 GPa respectively [19].

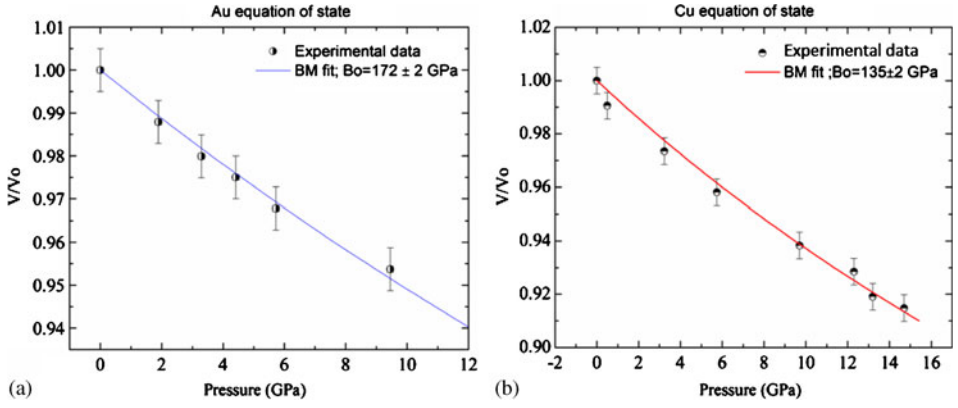

Figure 9. Equation-of-state of (**a**) Au and (**b**) Cu.

4.2 *High-pressure behaviour of sesquioxides (Dy_2O_3, Gd_2O_3, Yb_2O_3, Nd_2O_3)*

Depending on the ionic radius of rare-earth element, the rare-earth sesquioxides crystallize in three different structural forms, viz. cubic, monoclinic and hexagonal. Sesquioxides with larger ionic radii stabilize in hexagonal phase whereas for smaller ones, cubic phase is more stable. High-pressure studies on the cubic and hexagonal structured sesquioxide would provide further insight into the high-pressure structural behaviour of rare-earth sesquioxides. Therefore, we have carried out high-pressure experiments on cubic Dy_2O_3, Gd_2O_3, Yb_2O_3 and hexagonal Nd_2O_3. Our measurements at the EDXRD beamline showed structural transitions in all these sesquioxides. In particular, cubic phase was shown to transform to hexagonal phase through a monoclinic phase which is similar to the ambient monoclinic phase found in some sesquioxides. The hexagonal phase of Nd_2O_3 also shows phase transition to a monoclinic phase at ∼27 GPa (figure 10) but this phase has been shown to be different from the monoclinic phase found in the case of other cubic rare-earth sesquioxides [27].

4.3 *Planned additions*

As mentioned above, a KB mirror would be installed on this beamline to provide smaller gauge volume and thus studies at higher pressures. In addition, a high-temperature stage for heating the sample upto ∼1200°C is being installed. A closed cycle refrigerator (CCR) cryostat would provide the studies of the samples at low temperatures (∼10 K). It must also be noted that world over optimal usage of EDXRD beamline is facilitated through its

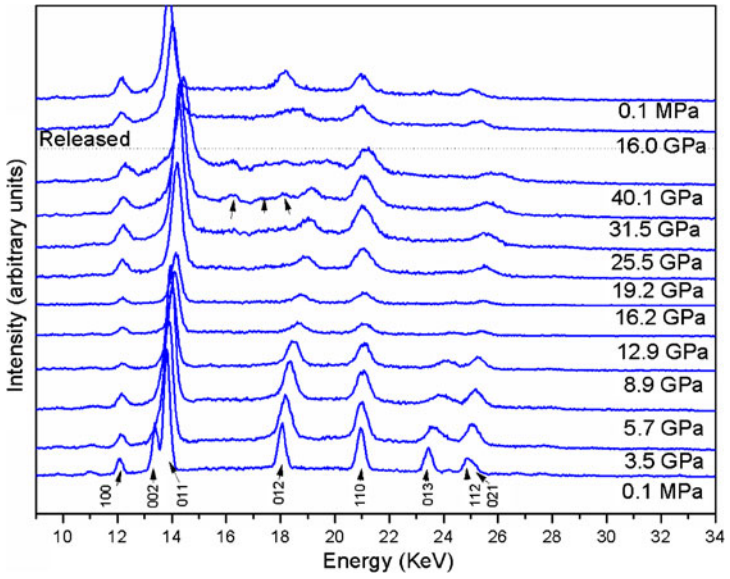

Figure 10. EDXRD patterns of Nd_2O_3 at different representative pressures.

installation at a powerful multipole wiggler source. In the same way, it is planned to have this beamline on a wiggler source once it becomes available at Indus-2.

5. Conclusions

An EDXRD beamline has been designed, developed and installed at BL-11 bending magnet port of the Indian synchrotron source, Indus-2. The beam has been optimized for carrying out structural investigations of materials under extreme conditions, viz. high-pressure. This beamline is operational and is now being routinely used. The sample stage at the experimental station has been designed to have high load capacity ($\sim$10 kg) which implies that other customized adaptations, for example high-temperature furnace, grazing incidence set-up etc., can also be incorporated to further enhance the capabilities of this beamline. Being equipped with energy-sensitive detector, this beamline can also be used for characterizing samples at ambient conditions using X-ray fluorescence.

Acknowledgements

Authors thankfully acknowledge the constant support and encouragement of Dr R K Sinha and Dr S Banerjee. Authors are also grateful to Dr P D Gupta and his colleagues from Synchrotron Utilization Division of RRCAT, Indore for providing the front-end for the beamline and A K Sinha and his colleagues from Centre for Design & Manufacture, BARC, for their help in the design and development of several components of the beamline.

References

[1] B E Warren, *X-ray diffraction* (Addison-Wesley, Reading, Massachusetts, 1969)
[2] B D Cullity, *Elements of x-ray diffraction*, 2nd edn (Addison-Wesley, Reading Massachusetts, 1978)
[3] E F Skelton, *Adv. X-ray Anal.* **31**, 1 (1988)
[4] B Buras and L Gerward, *Prog. Crystal Growth Charact.* **18**, 93 (1989)
[5] D Hausermann and P Barnes, *Phase Transitions* **39**, 99 (1992)
[6] B Buras and L Gerward, *International tables for crystallography*, 2nd edn, edited by A J C Wilson and E Prince (Kluwer Acad. Publ., Dordrecht, 1999) Vol. C, p. 87
[7] H Cole, *J. Appl. Cryst.* **3**, 405 (1970)
[8] Yejun Feng, R Jaramillo, G Srajer, J C Lang, Z Islam, M S Somayazulu, O G Shpyrko, J J Pluth, H-k Mao, E D Isaacs, G Aeppli and T F Rosenbaum, *Phys. Rev. Lett.* **99**, 137201 (2007)
[9] www.cat.gov.in/technology/accel/indus/indus2.html
[10] hpcat.gl.carnegiescience.edu/beamlines/bm-b
[11] www.spring8.or.jp/en/news_publications/publications/sp8_brochure/beamline.html
[12] www.helmholtz-berlin.de/index_en.html
[13] Helmut Wiedemann, *Synchrotron radiation* (Springer, 2003)
[14] R L Suthar and A K Sinha, *BARC News Lett.* **275**, 27 (2006)
[15] A Jayaraman, *Rev. Mod. Phys.* **55**, 65 (1983)
[16] R L Suthar and A K Sinha, *BARC News Lett.* **289**, 20 (2008)
[17] Paul Kirkpatrick and A V Baez, *J. Opt. Soc. Am.* **38**, 766 (1948)
[18] Roger J Dejus and Manuel Sanchez del Rio, *Rev. Sci. Instrum.* **67(9)**, 1 (1996)

[19] A Dewaele, P Loubeyre and M Mezouar, *Phys. Rev*. **B70**, 094112 (2004)
[20] H K Mao, P M Bell, J Shaner and D Steinberg, *J. Appl. Phys.* **49**, 3276 (1978)
[21] Debdutta Lahiri and Surinder M Sharma, BARC External Report No. BARC/2007/E/16
[22] H M Rietveld, *J. Appl. Cryst.* **2**, 65 (1969)
[23] A C Larson and R B Von Dreele, Los Alamos National Laboratory Report LAUR 86-748 (1994)
[24] A Le Bail, *Powder Diffraction* **20**, 316 (2005)
[25] A A Eliseev *et al*, *Kristallografiya* **31**, 803 (1986)
[26] F D Murnaghan, *Proc. Natl. Acad. Sci. USA* **30(9)**, 244 (1944)
[27] K K Pandey, Nandini Garg, A K Mishra and Surinder M Sharma, *J. Phys. Conf. Ser.* **377**, 012006 (2012)